

## Signature of present and projected climate change at an urban scale: The case of Addis Ababa



Bisrat Kifle Arsiso<sup>a,b</sup>, Gizaw Mengistu Tsidu<sup>c,\*</sup>, Gerrit Hendrik Stoffberg<sup>a</sup>

<sup>a</sup> Department of Environmental Science, University of South Africa (UNISA), South Africa

<sup>b</sup> Department of Environment and Climate Change, Ethiopian Civil Service University, Addis Ababa, Ethiopia

<sup>c</sup> Department of Earth and Environmental Sciences, Botswana International University of Technology and Science, Priv. Bag 16, Palapye, Botswana

### ARTICLE INFO

#### Keywords:

Addis Ababa-Ethiopia  
Climate change  
Emission scenarios  
Representative concentration pathways  
Urban climate

### ABSTRACT

Understanding climate change and variability at an urban scale is essential for water resource management, land use planning, development of adaption plans, mitigation of air and water pollution. However, there are serious challenges to meet these goals due to unavailability of observed and/or simulated high resolution spatial and temporal climate data. The statistical downscaling of general circulation climate model, for instance, is usually driven by sparse observational data hindering the use of downscaled data to investigate urban scale climate variability and change in the past. Recently, these challenges are partly resolved by concerted international effort to produce global and high spatial resolution climate data. In this study, the 1 km<sup>2</sup> high resolution NIMR-HadGEM2-AO simulations for future projections under Representative Concentration Pathways (RCP4.5 and RCP8.5) scenarios and gridded observations provided by Worldclim data center are used to assess changes in rainfall, minimum and maximum temperature expected under the two scenarios over Addis Ababa city. The gridded 1 km<sup>2</sup> observational data set for the base period (1950–2000) is compared to observation from a meteorological station in the city in order to assess its quality for use as a reference (baseline) data. The comparison revealed that the data set has a very good quality. The rainfall anomalies under RCPs scenarios are wet in the 2030s (2020–2039), 2050s (2040–2069) and 2080s (2070–2099). Both minimum and maximum temperature anomalies under RCPs are successively getting warmer during these periods. Thus, the projected changes under RCPs scenarios show a general increase in rainfall and temperatures with strong variabilities in rainfall during rainy season implying level of difficulty in water resource use and management as well as land use planning and management.

### 1. Introduction

A demographic change is taking place at a significant rate across the developing countries that will be expected to see an additional two billion residents in urban areas in the next 20 years, with the urban populations of Africa doubling through this period (UNDESA, 2009). This will certainly exacerbate the emissions of greenhouse gases which are found to contribute to a rise in global average surface temperature by about 0.9 °C–1.3 °C for the period 2016 to 2035 (Revi et al., 2014; Brian, 2009). It is now widely accepted that climate change has already occurred and further climate variability and change are inevitable (Solomon et al., 2007). For example, one of the results from Inter-governmental Panel on Climate Change (IPCC) WG-I 5th Assessment Report (AR5) shows that the world average surface temperature raised by 0.85 °C between 1880 and 2012 (Revi et al., 2014). Climate related risks due to increased variations in climate and weather associated with

extreme events have emerged as key natural hazards of the 21st century (Revi et al., 2014; Hayhoe and Gelca, 2013; Dastagir, 2015). Studies on both present climate variability and future climate change scenarios available today for assessing climate change impacts, vulnerability and adaptation have predominantly been derived from Global Circulation model (GCM) outputs. GCMs are the most multifaceted tools currently available for simulating the global climate system (Randall et al., 2007).

Various GCMs represent global climate in three dimensional-grids with horizontal resolution from 2.5° latitudes by 3.75° longitudes for atmospheric components to 1.25° Latitudes by 1.25° longitudes for oceanic components (Gordon et al., 2000). Recently, there is substantial improvements in the spatial resolution of GCMs despite computational costs and challenges in data storage. Yet, the information from GCMs may not be realistic for regional/national climate change impacts, adaptation and vulnerability assessments because of the high level of

\* Corresponding author.

E-mail addresses: [bisrat\\_k2002@yahoo.com](mailto:bisrat_k2002@yahoo.com) (B.K. Arsiso), [mengistug@biust.ac.bw](mailto:mengistug@biust.ac.bw) (G. Mengistu Tsidu).

uncertainty in GCM simulations due to their coarse grid resolution and the possible misrepresentation of local and meso-scale climate and hydrological processes (Nimusiima *et al.*, 2014). Previous studies have revealed that the model conformity with observations is the way to verify the quality of model (Houghton *et al.*, 2001). Moreover, the quality of model as assessed from the present climate assures the reliability of climate change simulations (Coquard *et al.*, 2004). Downscaling of GCMs is therefore essential and has been found to reduce the above and associated problems.

Statistical and dynamical downscaling are the two techniques normally used in climate research to obtain high resolution climate data. Dynamical downscaling involves nesting a Regional Climate Model (RCM) into a GCM which provides boundary as well as initial conditions (Christensen and Hewitson, 2007). Dynamical downscaling can simulate local feedback features which may not be captured by statistical methods, however, it requires strong computing resources. Statistical downscaling, on the other hand, involves finding statistical relationships between global scale features from GCMs and fine scale climate for a particular location which requires less computing resources and may be used to supplement intermediate dynamical downscaling (Mahmood and Babel, 2014).

As a result, these resource intensive GCMs simulations are produced by various international research centers through coordination with IPCC and made available to researchers. For example, the IPCC produced and encapsulated forty emission scenarios of regional and global path, based on different theory for processes such as growth of population, social and economic development, technology and energy development, land use change and agricultural development in 2000 (IPCC, 2000). The Special Report on Emission Scenarios (SRES) have been assessed critically in relation to the natural resource availability, use of economic parameters and production expectations in future in a number of studies that followed (IPCC, 2007; Parry *et al.*, 2007). For instance, the 4th assessment report of IPCC (AR4) used Special Report on Emission Scenarios (SRES) for the coupled model Inter-comparison project three (CMIP3) (Solomon *et al.*, 2007). However, the uncertainties in socioeconomic processes under SRES scenarios motivated the development of Representative Concentration Pathway (RCPs) scenarios that use greenhouse gases (GHGs) and radiative forcing. The RCPs give projections of indicators of climate and green house gas emissions, before starting from projections of socioeconomic processes or emission scenarios (Thoeun, 2015). An indicator of climate employed in RCPs comprises of greenhouse gases (GHGs) concentrations and radiative forcing in watts per square meter. The inclusion of adaptation, mitigations and climate policies in RCP makes the assessment of climate impacts potentially clearer (Van Vuuren *et al.*, 2011; Kumar *et al.*, 2012).

Climate projections for Ethiopia have been reported based on the CMIP3 models but with limited scope (NMA, 2007). Since then the improved set of emission scenarios (i.e., RCPs) are developed by the scientific community (Revi *et al.*, 2014). To our knowledge, there is no work based on the new scenarios with similar scope as the report based on SRES scenarios. Therefore, this study employed statistically down-scaled NIMR-HadGEM2-AO model data to study current and future climate change and variabilities at an urban scale for the city of Addis Ababa (Fig. 1). The downscaled and bias corrected NIMR-HadGEM2-AO model outputs for both present and future periods under RCP4.5 and RCP8.5 scenarios are constructed based on WorldClim reference climatology, which itself is constructed from observations, GPCC rainfall and CRU temperature. Worldclim is used for downscaling whereas GPCC rainfall and CRU temperature are used for bias correction. The WorldClim reference climatology is a high spatial resolution (about 1 km<sup>2</sup>) global climate set consisting of layers which are suitable to assess the climate of urban areas (Hijmans *et al.*, 2005). This spatial resolution is critically important as the Addis Ababa city is located in the highlands of Ethiopia which is very rugged and exhibits altitude variation from 2000 m in the south to over 3000 m in the north of the city

(Fig. 1).

The two (of the four) RCP scenarios used in this study are RCP4.5 and RCP8.5 as they represent optimal and extreme scenarios respectively. RCP4.5 is one of the modest scenarios in which radiative forcing becomes stabilized before 2100. RCP8.5 assumes the worst case scenario under which there will be least amount of effort in emissions reduction.

The paper is organized as follows. Descriptions of observational data, delta change method and NIMR-HadGEM2-AO model are given Section 2. A brief evolution of NIMR-HadGEM2-AO and its suitability for this study are also briefly described in Section 2. In Section 3 results and discussions on various aspect of historical and projected climate variability and change of the city are given. Finally, conclusions are presented in Section 4.

## 2. Data and methodology

### 2.1. Data

Observed daily and monthly historical data for rainfall, maximum temperature (Tmax) and minimum temperature (Tmin) at Addis Ababa Observatory station (9.01 °N, 38.74 °E) in the city were used. The NIMR-HadGEM2-AO model data for historical and projections under RCP 4.5 and RCP 8.5 are obtained from CMIP5 data server and then statistically downscaled using delta method. The data sets are selected because of their availability. Moreover, NIMR-HadGEM2-AO was developed by incorporating processes in the troposphere, land surface and hydrology, aerosols, ocean and sea ice in the course of several development phases. This version of the model is improved by including several changes and additions to the representation of aerosol. These include changes to existing aerosol species, such as sulphate and biomass-burning aerosols, and representation of additional species, such as mineral dust, fossil-fuel organic carbon, and secondary organic aerosol (The HadGEM2 Development Team: Martin and Coauthors, 2011). These changes improved the agreement in aerosol optical depth between model and observations (Bellouin *et al.*, 2007). The NIMR-HadGEM2-AO model also incorporates land use change applying Land-use Harmonization (LUH) (Hunt and Watkiss, 2011).

The gridded 1 km<sup>2</sup> resolution observed data set from Worldclim is used as a reference climatology for downscaling NIMR-HadGEM2-AO after validating it with station observation.

### 2.2. Methodologies

It is rather inappropriate to use spatial resolution of a GCM to provide features that are important to study climate impact at regional and local scale. To avoid such restriction, it is common to use down-scaled data from GCMs (Parry *et al.*, 2007). There are two techniques used in downscaling: dynamical and statistical. Statistical downscaling techniques develop relation between observed variable of local climate and GCM predictors. These relations are then used in the projections of future GCM to local climate variables (Samadi *et al.*, 2012). The delta method is used to downscale projections under RCP 4.5 and RCP 8.5 scenarios from NIMR-HadGEM2-AO model which are made available in the frame work of IPCC AR5. The gridded observations, also available at Worldclim data archive (Hijmans *et al.*, 2005), are used as a reference climatology in the statistical downscaling of the projections. The GCM data is first interpolated to the spatial scale of reference climatology using the thin-plate smoothing spline so that the reference monthly climatology is used at individual grid. The downscaled data sets have been subjected to bias correction using GPCC rainfall and CRU temperature.

The delta change method, which assumes that GCMs simulate relative changes more reliably than absolute values (Hay *et al.*, 2000; Tryhorn and DeGaetano (2011) and references therein), for temperature and precipitation are respectively given by

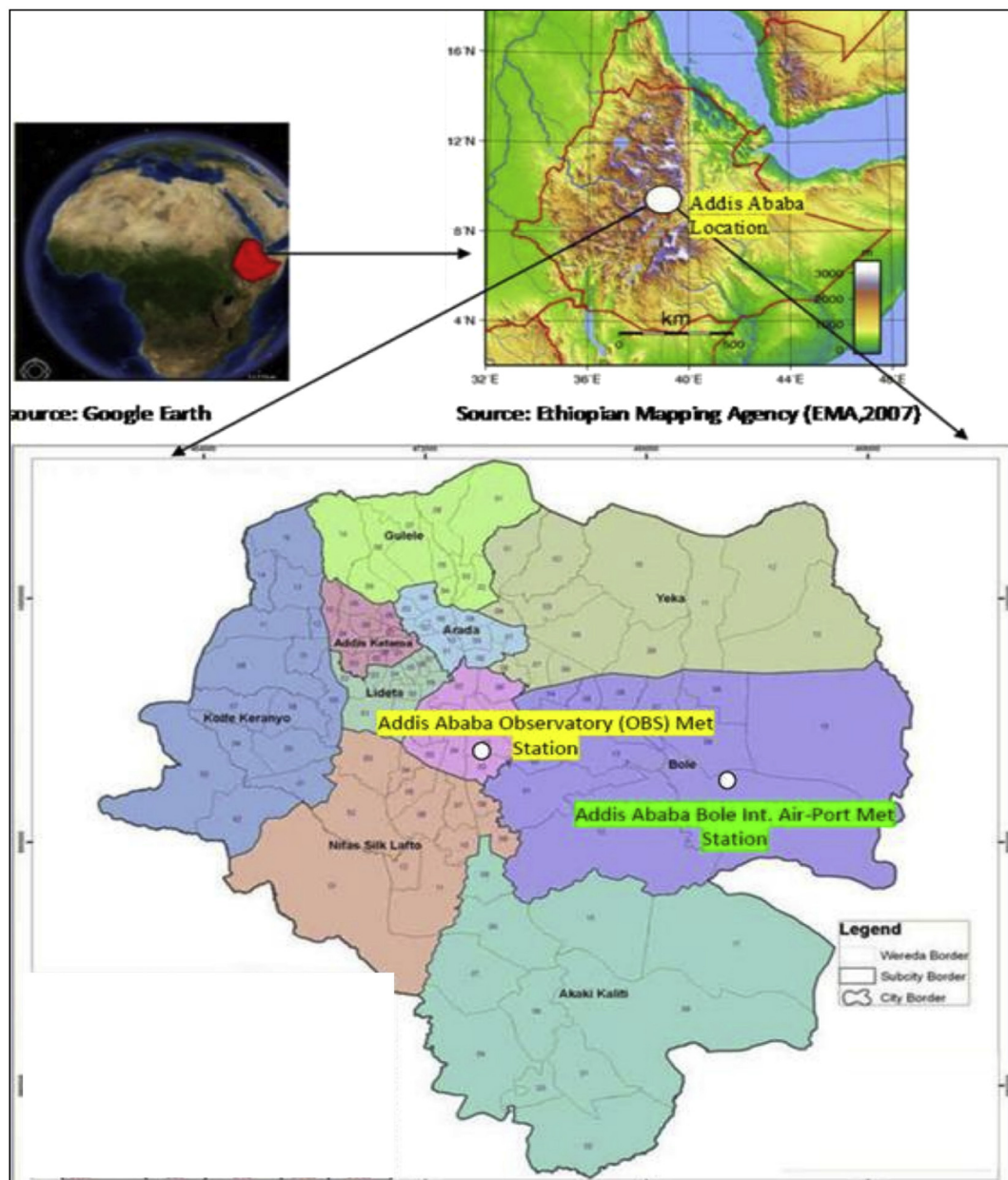


Fig. 1. The topography of the study area.

$$T_{deb} = T_{SCEN} - (\overline{T_{CURE}} - \overline{T_{OBS}}) \quad (1)$$

$$P_{deb} = P_{SCEN} \times \left( \frac{\overline{P_{OBS}}}{\overline{P_{CURE}}} \right) \quad (2)$$

where  $T_{deb}$  and  $P_{deb}$  are monthly time series of corrected temperature and precipitation for future periods while  $SCEN$  represents the downscaled scenario data for the future periods (e.g., 2006–2099), and  $CURE$  represents downscaled data for the observed period (e.g., 1950–2000). The bar on  $T$  and  $P$  shows the long-term average for each month. The monthly mean of 50 years (1950–2000) are deducted as given in Eqn. (1) for temperature. For precipitation long-term observed monthly mean rainfall data is divided by simulated rainfall as shown in Eqn. (2). The multiplicative factor in the case of precipitation are used for precipitation to avoid potential sign problems (i.e. the potential to calculate negative precipitation using an additive approach), and additive perturbations are used with temperature to avoid problems with temperature not being on an absolute scale. The factors are computed for each calendar month as the ratio or difference between the GCM and

observed values for the baseline period. The scaled values are expected to produce the fine scale spatial variability of the gridded observations. Many features of the original time series and spatial variability of the gridded observations are preserved by the delta method, and bias in the mean in the NIMR-HadGEM2-AO simulations is removed during the process. Changes in the seasonality of temperature and precipitation are captured, but with the same climate change perturbation. Thus, the bias corrected, large scale anomalies are used to estimate time series of monthly values at the fine grid scale. The assessment of climate change over the city is based on four climate periods, namely: current climate, and climates of the 2030s, 2050s and 2080s.

### 3. Results and discussions

#### 3.1. Current climate

##### 3.1.1. Observations

Fig. 2 depicts identifiable variability in rainfall and changes in

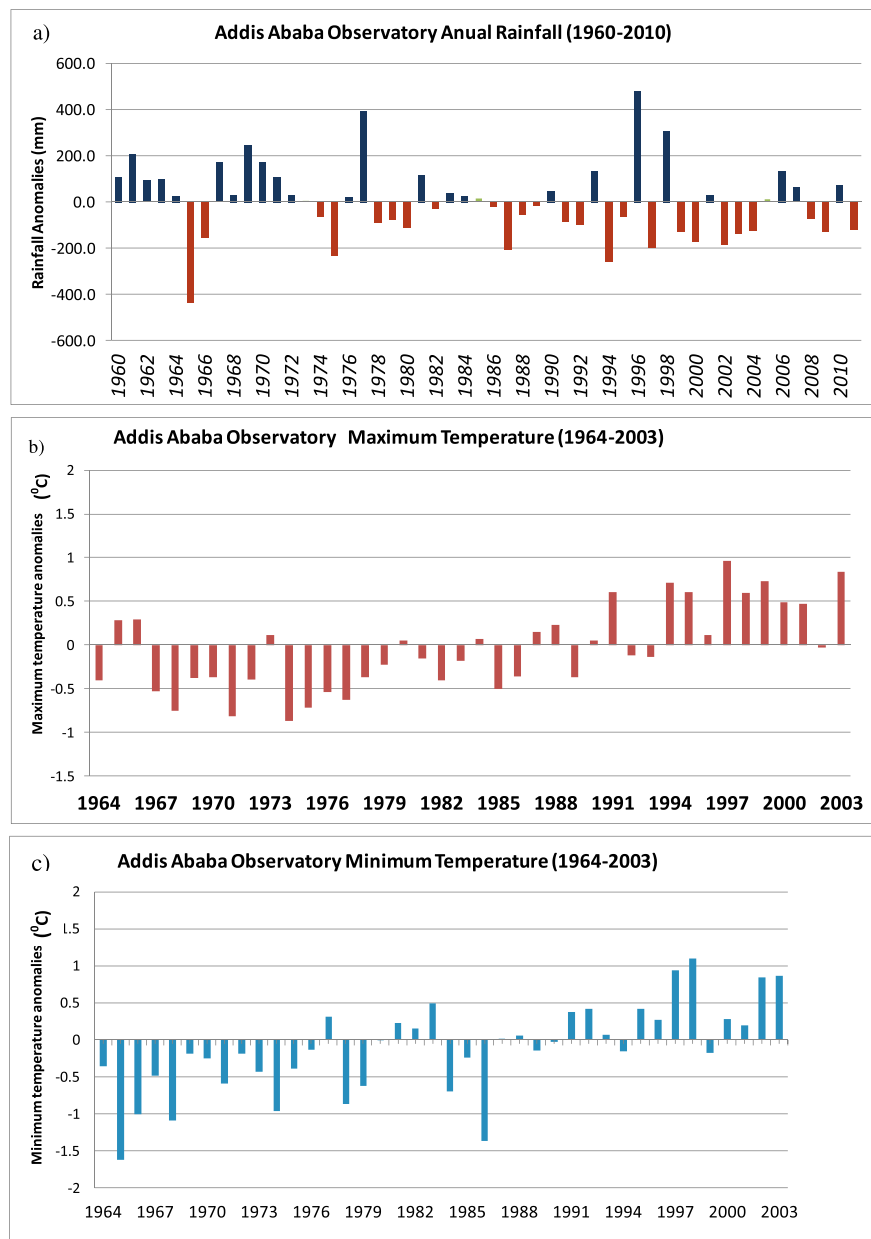


**Fig. 2.** Annual rainfall, minimum and maximum temperature anomalies compared to the 1971–2000 base period at Addis Ababa (Observatory) station.

temperatures over time. For precipitation, the late 1970s and most of the 1990s and the 2000s dry periods are clearly evident from several years of major annual departures. However, it was 1965 that witnessed the driest year on record (Fig. 2a). Periods of above average precipitation are also clearly evident in the historical record. For example, the annual rainfall in the 1969, 1977, 1996 and 1998 are well above average of the baseline mean. Notable warm periods in the city of Addis Ababa occurred in the 1990s and early 2000s (Fig. 2b–c). Since 1991 the average annual maximum temperature anomalies is about 0.5–1  $^{\circ}\text{C}$  above the average ( $24\text{ }^{\circ}\text{C}$ ) (1971–2000) (Fig. 2b–c). As a result, there is a clear warming trend of both minimum and maximum temperatures over the city center. The warming trend did not arise from purely the urban heat island effect since similar warming trend is observed at the outskirts of the city in the airport station. However, annual precipitation does not seem to have a discernible trend.

Fig. 3 shows mean climatology of rainfall, maximum and minimum temperatures as revealed from station observation and gridded observational dataset of WorldClim data for the 1950–2000 base period.

The comparison of gridded observation from WorldClim for the baseline period and observations at Addis Ababa Observatory shows excellent agreements for all variables (rainfall (Fig. 3a), and minimum and maximum temperature (Fig. 3b)). There is a minor difference between gauge rainfall from the station and gridded rainfall from Worldclim during main rainy season from June to September (Fig. 3a). The Worldclim rainfall is slightly dry biased with respect to observation at the station. The gridded minimum and maximum temperature are systematically lower than temperature at the stations throughout the whole seasons but the departure is in the order of 1  $^{\circ}\text{C}$  for maximum temperature and far less for the minimum temperature. These discrepancies, which are quite small, are likely attributable to errors that arise from gridding of sparse data over the region as noted in previous study for a different data (Mengistu Tsidu, 2012).

Fig. 4 shows observed WorldClim data for the baseline mean of minimum and maximum temperatures (Fig. 4a–b), rainfall (Fig. 4c) and seasonal distribution of rainfall at seven sub-cities of Addis Ababa (Fig. 4d). Addis Ababa city is located in central plateau of Ethiopia with

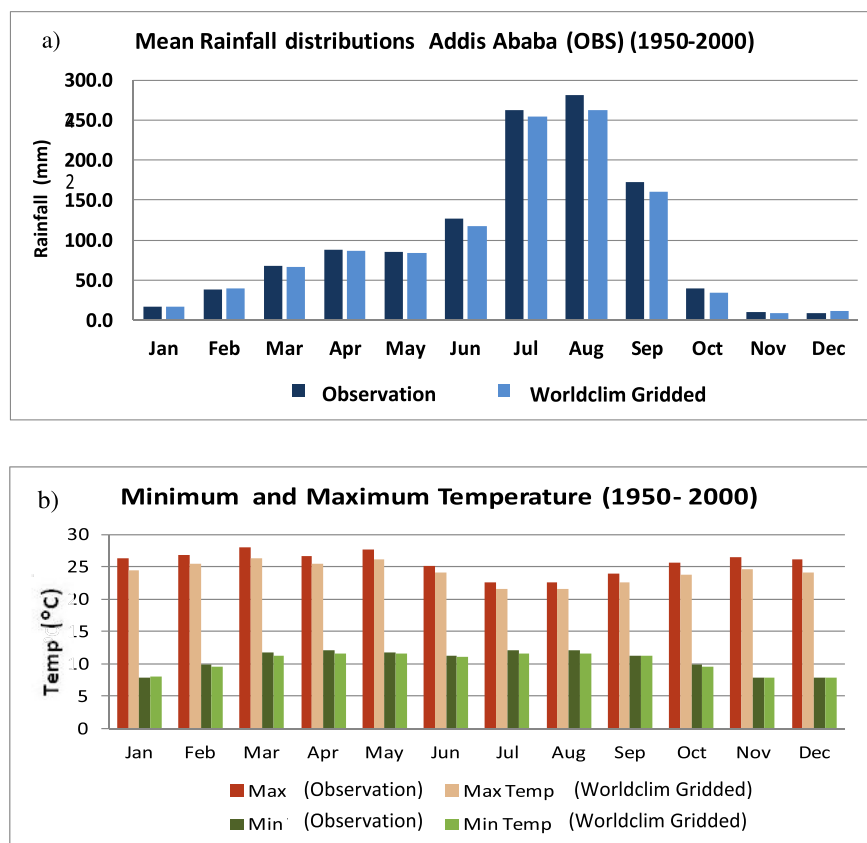


Fig. 3. The baseline mean climatology of WorldClim data (1950–2000) and observation at the Addis Ababa Observatory station as shown in the figure legends.

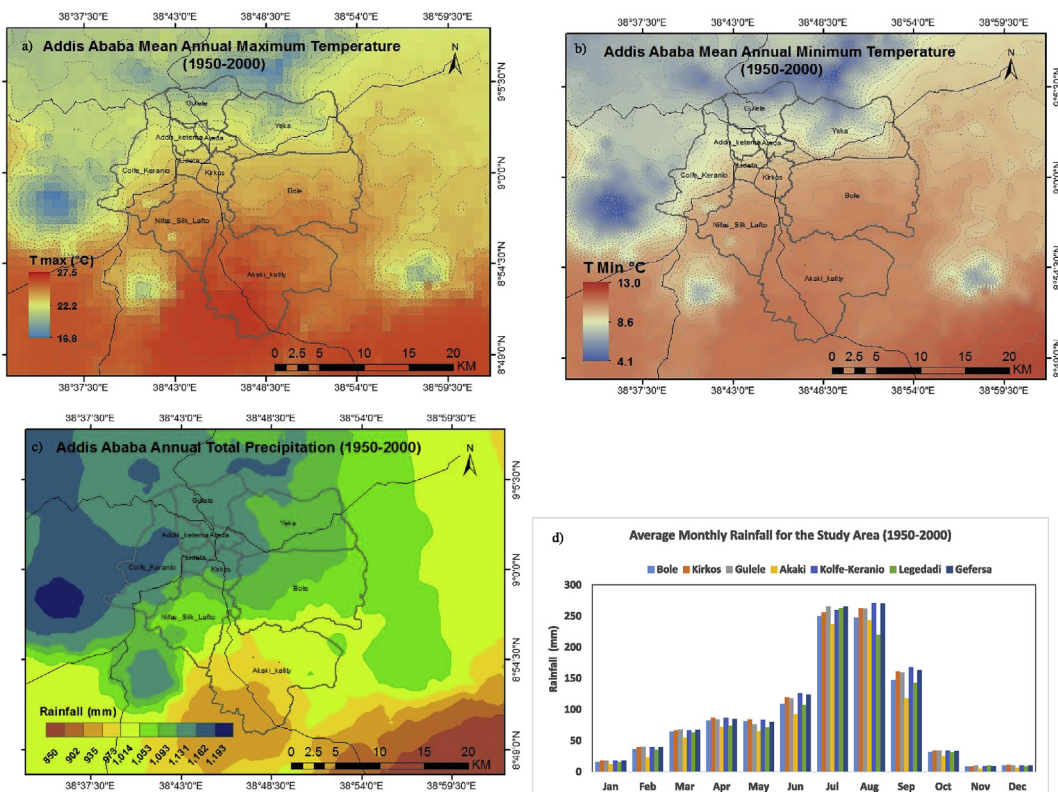
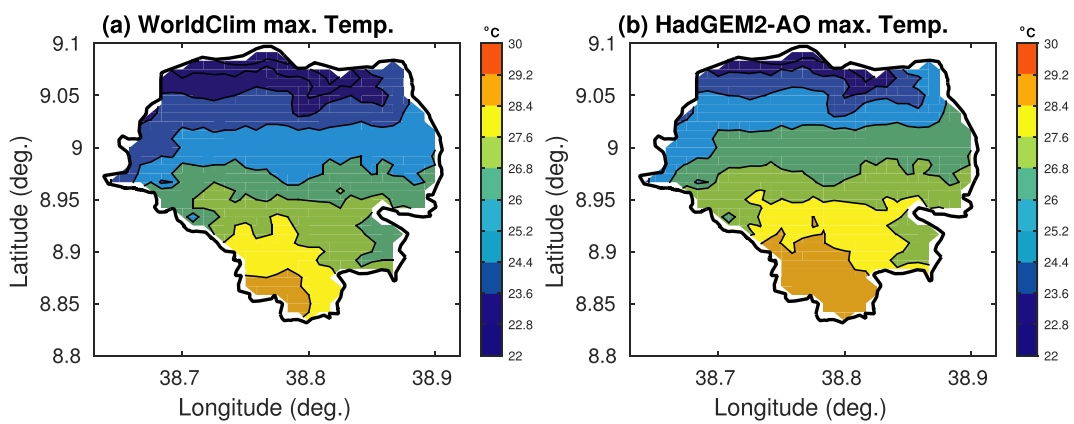
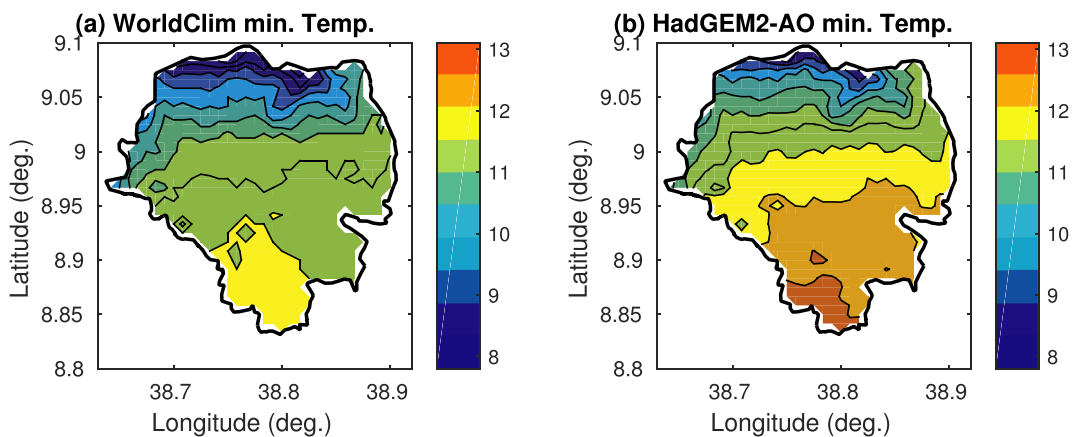


Fig. 4. Historic mean annual (1950–2000) maximum (a) and minimum temperature (b) and annual total precipitation (c) over Addis Ababa and surrounding areas from WorldClim data set.



**Fig. 5.** Comparison of WorldClim historic mean annual maximum (a) and downscaled and bias corrected simulation of NIMR-HadGEM2-AO historic mean annual (1950–2000) maximum (b) temperatures over Addis Ababa and surrounding areas.



**Fig. 6.** Comparison of WorldClim historic mean annual minimum (a) and downscaled and bias corrected simulation of NIMR-HadGEM2-AO historic mean annual (1950–2000) minimum (b) temperatures over Addis Ababa and surrounding areas.

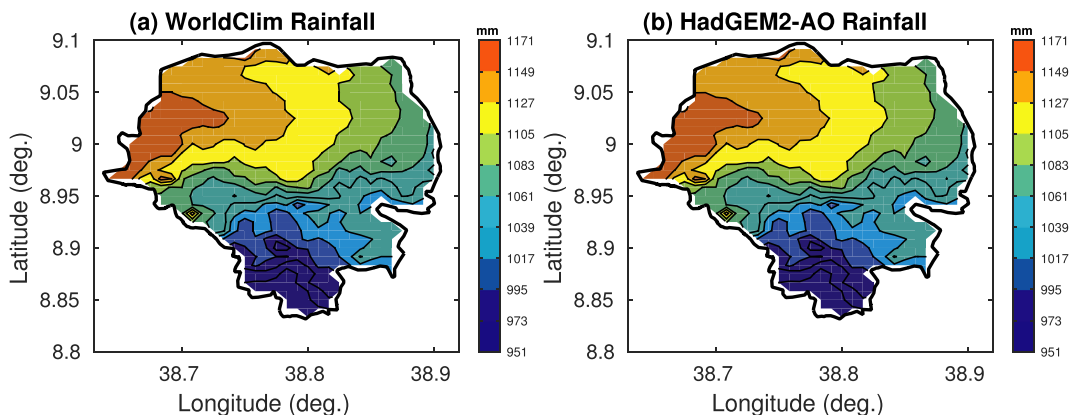


**Fig. 7.** Comparison of WorldClim historic mean annual rainfall (a) and downscaled and bias corrected simulation of NIMR-HadGEM2-AO historic mean annual (1950–2000) rainfall over Addis Ababa and surrounding areas.

significant variation in elevation (from over 3000 m in the north to about 2050 m in the south of the city). This natural landscape modulates pressure, temperature, precipitation and wind patterns. As a result, over a relatively short distance from Entoto and Menagesha Suba mountains area in the north to Akaki Sub-city in the south, there is an increase in maximum temperature with decrease in elevation (Fig. 4a). Likewise, minimum temperature decreases from north, Gulele and Yeka sub-cities, to south, Akaki sub-city. Unlike maximum temperature, the north-south minimum temperature gradient is not linear (Fig. 4b) as the urban heat island effect offsets the altitude effect.

Rainfall decreases dramatically from the high lying parts of the city in the northwest to the low lying Akaki Kality sub-city in the south with gradient oriented along approximately northwest-southeast direction (Fig. 4c). The mean annual total rainfall varies spatially from 935 to 1162 mm across a distance of about 30 km (Fig. 4c). The seasonal distributions of rainfall at seven locations representing the sub-cities are the same except during summer (June to September). The significant differences between sub-cities are observed in August rainfall as characterized by high rainfall observed at Kolfe-Keranio and Gefersa against low rainfall at Legedadi and Akaki sub-cities (Fig. 4d). This reveals that

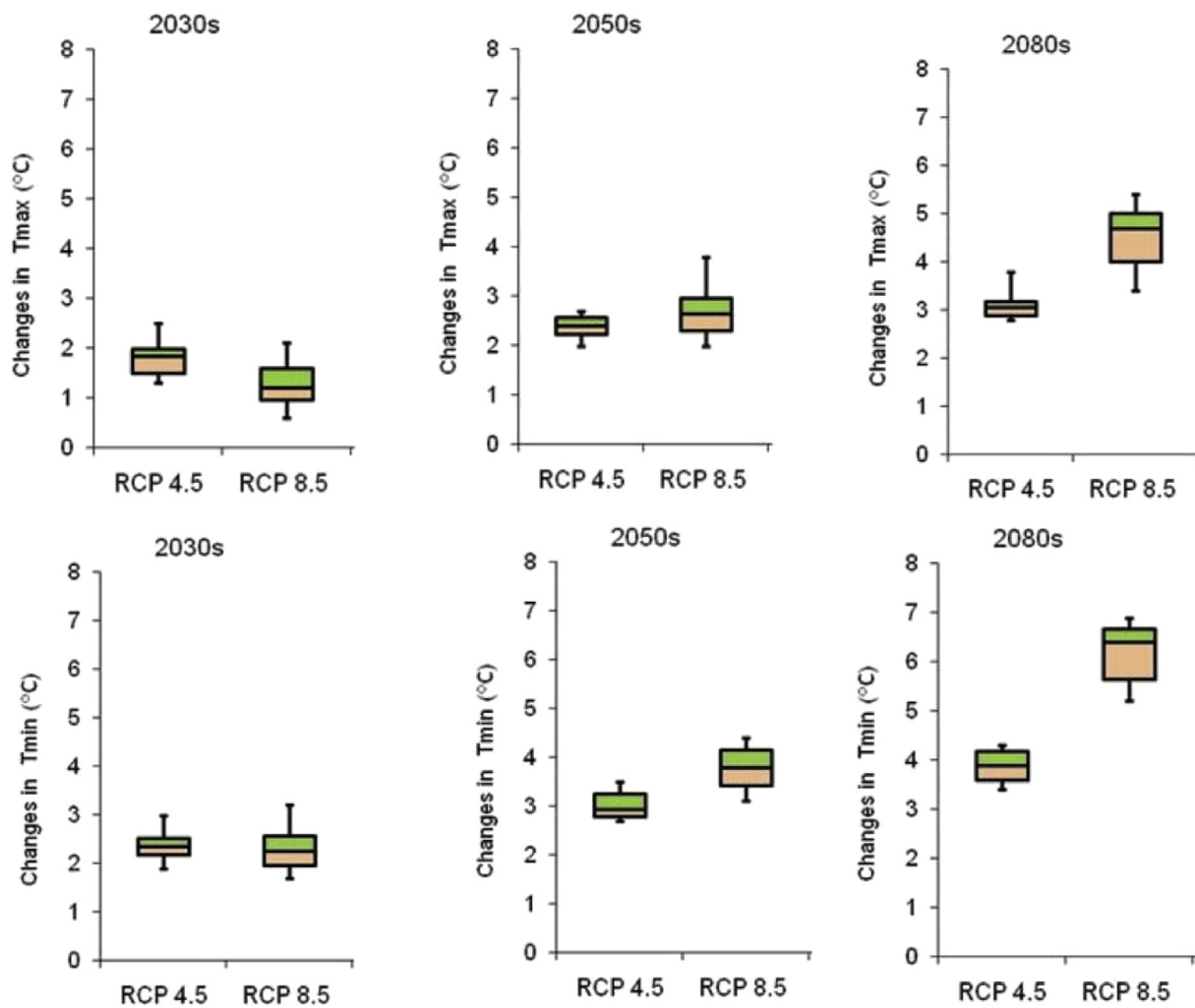


Fig. 8. Box plot for the mean annual changes in maximum and minimum temperature in the 2030s 2050s, and 2080s.

the northwest-southeast rainfall gradient of the mean annual total comes mainly from the rainfalls during summer.

### 3.1.2. NIMR-HadGEM2-AO simulations

In order to use NIMR-HadGEM2-AO simulations to characterize climate change and variability at an urban scale, a number of assessments have to be made on the quality of data used for downscaling and bias correction. Moreover, the downscaled data set has to be also evaluated with respect to its comparability with observations during historical periods. It has already been shown in Section 3.1.1 that the high resolution WorldClim temperature and rainfall data are able to capture observations at the center of the city remarkably well. In this Section, assessment of downscaled and biased corrected NIMR-HadGEM2-AO in depicting comparable spatial variability as the Worldclim is made.

Fig. 5 shows the Worldclim annual mean maximum temperature (Fig. 5a) and downscaled and bias correction model simulation (Fig. 5b). Linear north-south spatial gradient with a correct sign is exhibited in both data sets. Moreover, the agreement is excellent over the extreme north and south. However, there is a difference in the range of 1–2 °C over wider areas in the central part of Addis Ababa.

The difference between Worldclim and NIMR-HadGEM2-AO minimum temperature is about 1 °C over central Addis Ababa while the two data sets show excellent agreement over the rest of the country (Fig. 6). Although both data sets exhibit north-south temperature gradients as exhibited from the altitude variation, the model minimum

temperature shows sharp and distinct gradient with distance.

The rainfall spatial patterns appear to be the same almost everywhere (Fig. 7). However, NIMR-HadGEM2-AO rainfall exhibits a wet bias of upto 0.4 mm over the eastern half of the city and a dry bias of about 0.6 mm over western half. The excellent agreement is naturally excepted since the same data was used in the downscaling of the GCM. However, the fact that the bias correction used different data sets from CRU for temperature and GPCC for rainfall could be a possible source of differences.

### 3.2. Climate projections under the RCPs scenarios

The outputs from NIMR-HadGEM2-AO climate model have already been bias-corrected under a mid-range RCP4.5 and a high emission RCP8.5 scenarios (Ariso et al., 2017). The data covers the period from January 1, 1950 to December 2099. The climatic baseline is chosen to cover the 1950–2000 period for evaluation of the projected changes in the mean annual and seasonal precipitation, maximum and minimum temperatures. A 50-year data meets the requirements for the baseline period recommended by IPCC (2007).

#### 3.2.1. Spatially averaged change in maximum and minimum temperatures

The box-plots (Fig. 8) shows that annual change of mean maximum and minimum temperatures of NIMR-HadGEM2-AO during the 2030s, 2050s, and 2080s with respect to the baseline mean under both RCP4.5 and 8.5 scenarios. Both projections indicate increase in maximum and

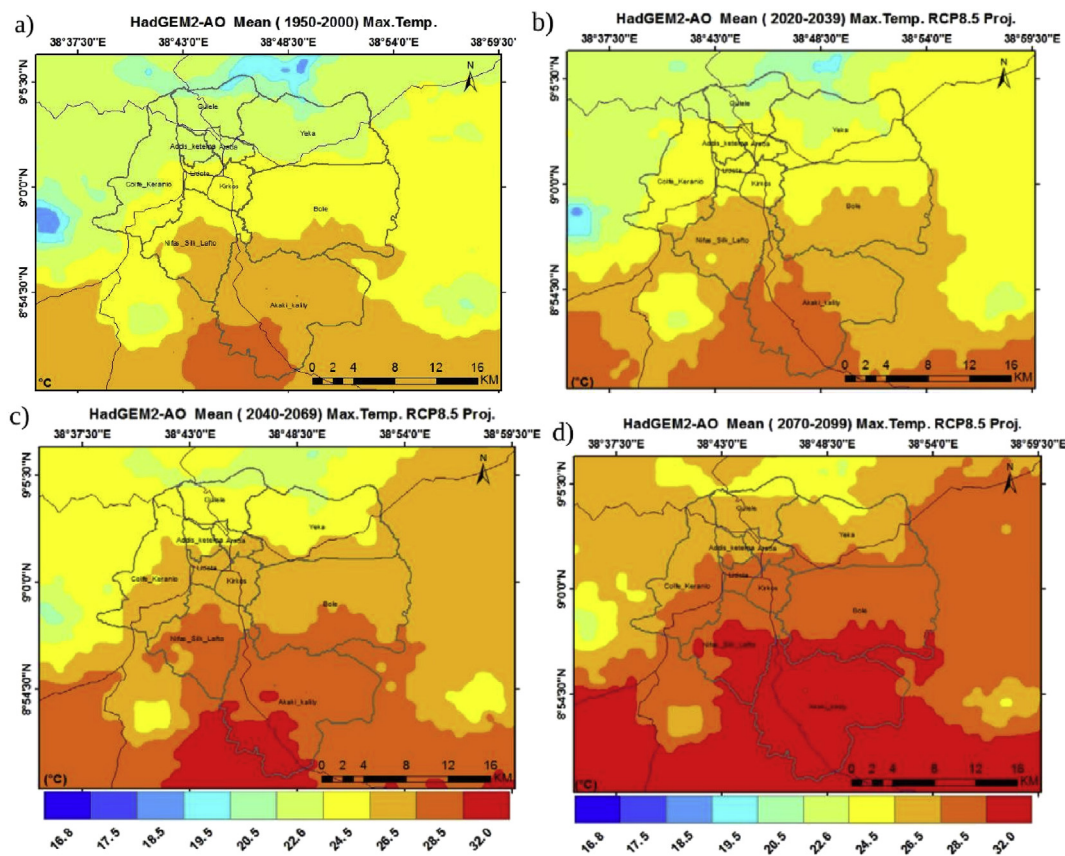


**Fig. 9.** The NIMR HadGEM-AO base period and projected mean maximum temperature during (a) base period and (b) the 2030s; (c) the 2050s and (d) the 2080s over Addis Ababa, Ethiopia under RCP 8.5 scenario.

minimum temperature for all three future periods. It is also evident that from whiskers of the box-plots that the range of change in annual temperature will increase with the time horizon. The middle 50% range of the box represents median values. The two ends of whiskers represent the extremes projection. The changes in annual maximum and minimum temperature projections under RCP8.5 are higher than RCP4.5 in all periods with the exception of the 2030s maximum temperature.

The mean annual maximum temperature anomalies under RCP 8.5 scenario exhibited an increase of 1.3–1.5 °C during the 2030s, 2.0–3.0 °C during the 2050s and 4.0–5.0 °C in the 2080s whereas projection under RCP 4.5 scenario shows increase by about 1.5–2.5 °C during the 2030s, 2.2–2.6 °C during the 2050s and 3.0 °C during the 2080s (Fig. 8). On other hand, projected change under RCP8.5 indicates that minimum temperature anomalies shows an increasing trend of about 2.0–2.6 °C in the 2030s, 3.5–4.2 °C during the 2050s and 5.5–6.7 °C during the 2080s under the RCP 8.5 scenario (Fig. 8). Similarly, the minimum temperature exhibits an increase from about 2.5 to 4 °C between the 2030s and 2080s.

### 3.2.2. Spatiotemporal change in maximum and minimum temperatures

The RCP 8.5 scenario shows an increase in future maximum temperature by about 1–2 °C for the entire city and surrounding areas through 2030s, with the highest change stretching along the Bole, Yeka, and Akaki sub-cities in the eastern and southern parts of the city (see Fig. 9a and b for comparison). In the 2050s (Fig. 9c), the maximum temperature has increased by 2–4 °C above the baseline mean (Fig. 9a). By 2080s, average maximum temperatures are projected to increase by about 3–6 °C over the same areas (Fig. 9d) above the average of the baseline period (Fig. 9a).

In general, Fig. 9 shows a steady increase in the mean maximum

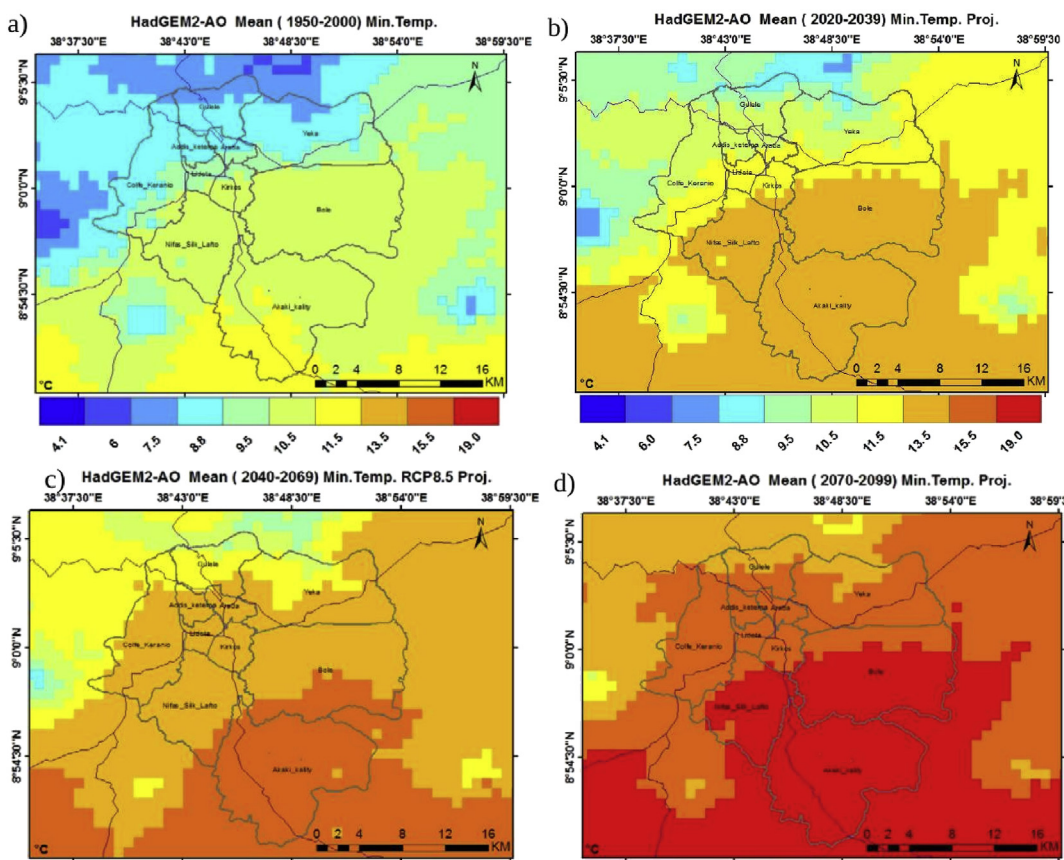
temperature with respect to the base period mean in time from near term in the 2030s to end term in the 2080s. For example, the highest maximum temperature of about 28.5 °C over southern part of the city during the base period (1950–2000) (Fig. 9a) has increased to 32 °C (Fig. 9d). This trend in maximum temperature change over southern part of the city is more amplified over the northern part of the city with increasing altitude.

Fig. 10 shows the simulated mean minimum temperature during the 1950–2000, 2030s, 2050s and 2080s. The simulation under RCP 8.5 scenario shows increase in future minimum temperature for the three future time periods since there is a clear expansion in the Akaki and Bole sub-cities (see Fig. 10b–d). These areas of the city are expected to experience the highest changes in minimum temperature in clear contrast to the maximum temperature change, suggesting that a minimum temperature is more sensitive to climate change. This is consistent with previous works in the literature (Lobell et al., 2007).

The changes in minimum temperature over the city is enormous in contrast to maximum temperature. For example, for the same southern part of the city, the minimum temperature increases from 11.5 °C during base period (Fig. 10 a) to 19.0 °C during the 2080s (Fig. 10 d). The amplification of minimum temperature change with increasing altitude is also apparent along north-south transect confirming the existing understanding that high altitude areas are more sensitive to climate change.

### 3.2.3. Spatiotemporal change in rainfall

Increase in rainfall is also expected over the city with time but the rate of change is higher over the northern part than over the southern part of the city (Fig. 11) in general. For example, the mean annual rainfall increases by about 100 mm in the 2030s (Fig. 11b) from about 1150 mm during the baseline period (Fig. 11a) over the northern part of



**Fig. 10.** The NIMR HadGEM-AO base period and projected mean minimum temperature during (a) base period and (b) the 2030s; (c) the 2050s and (d) the 2080s over Addis Ababa, Ethiopia under RCP 8.5 scenario.

the city. In contrast, the increase over southern part of the city is in the range of 150–200 mm (Fig. 11b) above the mean of baseline. The rainfall in the 2050s remains almost the same as that of 2030s over northern part of the city while it exhibits significant increase of about 200–260 mm above the baseline period mean (Fig. 11c). The increase in rainfall in the 2080s over the northern and southern parts of the city is about 200 mm and in the range of 280–350 mm (Fig. 11d) above the baseline mean of 1050 mm and 950–1050 mm (Fig. 11a) respectively. In general, the future climate in the Addis Ababa and the surrounding areas is expected to be wetter under the RCP 4.5 (not shown) and RCP 8.5 scenarios. The upward trend in rainfall is likely to affect water catchment area positively.

#### 4. Conclusions

Analysis of observations at the city center indicates existence of identifiable variability in rainfall and changes in temperatures over time. The notable warm periods in the city of Addis Ababa in the 1990s and early 2000s, the dry periods of the 1970s, 1990s and 2000s; as well as the above normal rainfalls during some years are clearly evident from the anomalies with respect to the selected baseline period. The mean climatology of gridded observed rainfall, maximum and minimum temperatures obtained from WorldClim data center are in good agreement with observed climatology at Addis Ababa Observatory for the same baseline period. The downscaled and bias corrected GCM simulations show considerable agreements with gridded reference monthly climatology which is already in agreement with observation from the synoptic meteorological station.

Two future scenarios are considered in this study to assess the climate variability and change at urban scale. The change in rainfall, maximum and minimum temperature over Addis Ababa city and its

surrounding is determined for three selected future periods with respect to the baseline period that extends from 1950 to 2000 under the two scenarios. The three future periods are the near term (2030s), midterm (2050s) and end term (2080s).

The departure of rainfall over Addis Ababa from baseline mean during future periods shows wet trend generally under both representative concentration pathways. However, the rainfall anomalies are higher under RCP8.5 than RCP4.5 with significant difference during mid and end terms.

The downscaled HadGEM2-AO maximum and minimum temperature show warming trend over Addis Ababa city under both RCP4.5 and RCP8.5 scenarios. However, change in minimum temperature is higher than maximum temperature. The later is consistent with existing literature. Moreover, the change in minimum temperature is high under RCP8.5 as compared to change under RCP4.5. The overall average temperature is warmer under RCP8.5 than under RCP4.5. This is consistent with expected wetter condition under RCP8.5 than under RCP4.5.

In short, the study has brought a number of evidences for existence of climate change signal at an urban scale with implications for water resource use and management as well as land use planning and management. The authors have conducted a couple of parallel studies to understand the implications of these changes at urban scale for water resource and land use management (Ariso *et al.*, 2017, 2018). Moreover, this study can be expanded to include more models available in the framework of IPCC CMIP5 at other urban sites in the African continent to gain further insights and estimates of uncertainty in the climate change signal.

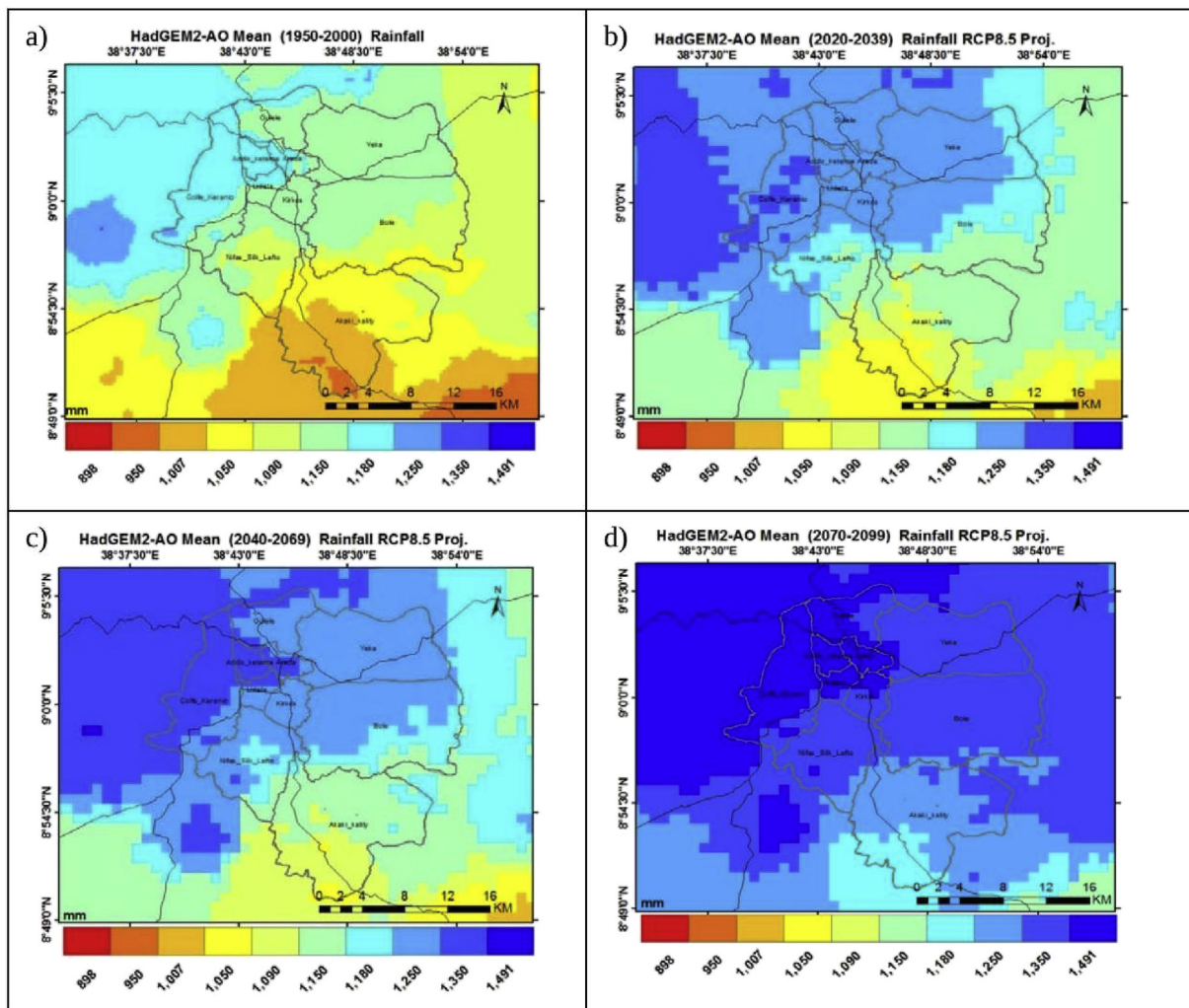


**Fig. 11.** The NIMR HadGEM-AO base period and projected mean annual rainfall during (a) base period and (b) the 2030s; (c) the 2050s and (d) the 2080s over Addis Ababa, Ethiopia under RCP 8.5 scenario.

## Acknowledgments

This study is part of the first authors doctoral research work at the University of South Africa (UNISA). The first author wishes to acknowledge and offer gratitude to the Ethiopian Civil Service University for the sponsorship of the doctoral study at UNISA. The corresponding author (GMT) acknowledges the Humboldt Foundation for the financial support through the Humboldt fellowship during which this work was initiated. The authors would also like to extend their heart-felt gratitude to the National Meteorological Agency (NMA) of Ethiopia for providing valuable data for the research as well as the WorldClim data archive center for providing high resolution climate data.

## References

Ariso, B., Mengistu Tsidu, G., Stoffberg, G., Tadesse, T., 2017. Climate change and population growth impacts on surface water supply and demand of addis ababa, Ethiopia. *Clim. Risk Manag.* 18, 21–33. <https://doi.org/10.1016/j.crm.2017.08.004>.

Ariso, B., Mengistu Tsidu, G., Stoffberg, G., Tadesse, T., 2018. Influence of urbanization-driven land use/cover change on climate: the case of addis ababa, Ethiopia. *Phys. Chem. Earth Parts A/B/C.* <https://doi.org/10.1016/j.pce.2018.02.009>.

Bellouin, N.O.B., Haywood, J., Johnson, C., Jones, A., Rae, J., Woodward, S., 2007. Improved Representation of Aerosols for HadGEM2. Hadley Centre Technical Note 73. Met Office Hadley Centre, Exeter, EX1 3PB, UK available from: <http://www.metoffice.gov.uk/learning/library/publications/science/climate-science>.

Brian, L., 2009. Climate Change in Park City: an Assessment of Climate, Snowpack, and Economic Impacts. Stratus Consulting Inc., Ste. 420 Washington, DC 20036.

Christensen, J., Hewitson, B.C., 2007. Regional Climate Projections. *IPCC WG1 Fourth Assessment Report.*

Coquard, J., Duffy, P., Taylor, K., Iorio, J., 2004. Present and future surface climate in the western USA as simulated by 15 global climate models. *Clim. Dynam.* 23, 455–472.

Dastagir, M., 2015. Modeling recent climate change induced extreme events in Bangladesh. *J. Weather Clim. Extremes* 7, 49–60.

Gordon, C., Cooper, C., Senior, C., Banks, H., Gregory, J., Johns, T., Wood, R., 2000. The simulation of sst, sea ice extents and ocean heat transports in a version of the hadley centre coupled model without flux adjustments. *Clim. Dynam.* 16 (2/3), 147–168.

Hay, L.E., Wilby, R.L., Leavesley, G.H., 2000. A comparison of delta change and down-scaled gcm scenarios for three mountainous basins in the United States. *JAWRA J. Am. Water Resour. Assoc.* 36, 387–397. <http://dx.doi.org/10.1111/j.1752-1688.2000.tb04276.x>.

Hayhoe, K.A.S., Gelca, R., 2013. *Climate Change Projections and Indicators for Delaware.* ATMOSResearch and Consulting.

Hijmans, R., Cameron, S.E., Parra, J.L., Jones, P.G., Jarvis, A., 2005. Very high resolution interpolated climate surfaces for global land areas. *Int. J. Climatol.* 25, 1965–1978.

Houghton, J., Ding, Y., Griggs, D.J., Noguer, M.V., Linden, P.J., Dai, X., Maskell, K., Johnson, C.A., 2001. *Climate Change: the Scientific Basis. Contribution of Working Group I to the Third Assessment Report of the Intergovernmental Panel on Climate Change(IPCC).* Cambridge University Press, Cambridge, UK/New York, USA.

Hunt, A., Watkiss, P., 2011. Climate change impacts and adaptation in cities: a review of the literature. *Clim. Change* 104 (1). <http://dx.doi.org/10.1007/s10584-010-9975-6>.

IPCC, 2000. *A Special Report on Emission Scenarios: a Special Report of Working Group III of the Intergovernmental Panel on Climate Change.* Cambridge University Press, Cambridge, UK.

IPCC, 2007. *Climate Change: the Scientific Basis. Contribution of Working Group I to the Third Assessment Report of the Intergovernmental Panel on Climate Change(IPCC).* Cambridge University Press, Cambridge, UK/New York, USA.

Kumar, R., Joshi, J., Jayaraman, M., Bala, G., Ravindranath, N.H., 2012. Multi-model climate change projections for India under representative concentration pathways. *J. Curr. Sci.* 103 (7).

Lobell, D., Bonfils, C., Duffy, P.B., 2007. Climate change uncertainty for daily minimum and maximum temperatures: a model inter-comparison. *J. Geophys. Res.* 112, L05715.

Mahmood, R., Babel, S.M., 2014. Future changes in extreme temperature events using the statistical downscaling model (sdsm) in the trans-boundary region of the jhelum river basin. *J. Weather Clim. Extremes* 5–6, 56–66.

Mengistu Tsidu, G., 2012. High-resolution monthly rainfall database for Ethiopia: homogenization, reconstruction, and gridding. *J. Clim.* 25, 8422–8443.

Nimusima, A., Basalirwa, C., Majaliwa, J., Mbogga, S.M., Mwavu, E., Namaalwa, J., Okello, J., 2014. Analysis of future climate scenarios over central Uganda cattle corridor. *J. Earth Sci. Clim. Change* 2157–7617.

NMA, 2007. Climate Change National Adaptation Programme of Action (NAPA) of Ethiopia. The World Bank.

Parry, M., Canziani, O.F., Palutik, J.P., Linden, P.J., Hanson, C.E., 2007. Contribution of Working Group II to the Fourth Assessment Report of the Intergovernmental Panel on Climate Change(IPCC). Cambridge University Press, Cambridge, UK.

Revi, A., Satterthwaite, D.E., Aragón-Durand, F., Corfee-Morlot, J., Kiunsi, R.B.R., Pelling, M., Roberts, D.C., Solecki, W., 2014. Urban areas. In: Field, C.B., Barros, V.R., Dokken, D.J., Mach, K.J., Mastrandrea, M.D., Bilir, T.E., Chatterjee, M., Ebi, K.L., Estrada, Y.O., Genova, R.C., Girma, B., Kissel, E.S., Levy, A.N., MacCracken, S., Mastrandrea, P.R., White, L.L. (Eds.), *Climate Change 2014: Impacts, Adaptation, and Vulnerability. Part A: Global and Sectoral Aspects. Contribution of Working Group II to the Fifth Assessment Report of the Intergovernmental Panel on Climate Change*. Cambridge University Press, Cambridge, United Kingdom and New York, NY, USA, pp. 535–612.

Randall, A., Wood, R., Bony, S., Colman, R., Fichefet, T., Fyfe, J., Taylor, E., 2007. *Climate Models and Their Evaluation*. Cambridge University Press, Cambridge, UK.

Samadi, S., Carbone, G.J., Mahdavi, M., Sharifi, F., Bihamta, M.R., 2012. Statistical downscaling of climate data to estimate stream-flow in a semi-arid catchment. *J. Hydrol. Earth Syst. Sci. Discuss.* 9, 4869–4918.

Solomon, S., Gian-Kasper, P., Reto, K., Pierre, F., 2007. Irreversible climate change due to carbon dioxide emissions. *Int. J. Environ. Sci.* 106 (6), 1704–1709.

The HadGEM2 Development Team Martin, G. M., Coauthors, 2011. The hadgem2 family of met office unified model climate configurations. *Geosci. Model Dev. Discuss. (GMDD)* 4, 765–841. <http://dx.doi.org/10.5194/gmdd-4-765-2011>.

Thoeun, H.C., 2015. Observed and projected changes in temperature and rainfall in Cambodia. *J. Weather Clim. Extremes* 7, 61–71.

Tryhorn, L., DeGaetano, A., 2011. A comparison of techniques for downscaling extreme precipitation over the northeastern United States. *Int. J. Climatol.* 31, 1975–1989. <http://dx.doi.org/10.1002/joc.2208>.

UNDESA, 2009. *World Population Prospects. The 2009 Revision Highlights, ESA/P/ WP.202*. The United Nations Department of Economic and Social Affairs, United Nations Press, New York.

Van Vuuren, D., Edmonds, J., Kainuma, M., Riahi, K., Thomson, A., Hibbard, K., Hurtt, G., Kram, T., Krey, V., Lamarque, J.F., Masui, T., Meinshausen, M., Nakicenovic, N., Smith, S., Rose, S., 2011. The representative concentration pathways: an overview. *Clim. Change* 109 (1), 5–31.